Journal of Biomechanics ∎ (∎∎∎∎) ∎∎∎–∎∎∎

JOURNAL OF BIOMECHANICS

www.elsevier.com/locate/jbiomech
www.JBiomech.com

Short communication

Predictions of bone remodeling around dental implant systems

Hsuan-Yu Chou, John J. Jagodnik, S. Müftü*

Department of Mechanical Engineering, Northeastern University, 360 Huntington Avenue, Boston, MA 02115, USA

Accepted 31 January 2008

Abstract

This study presents the implementation of a mathematical bone remodeling algorithm to bone adaptation in the premolar area of the mandible around various dental implant systems, and thus sheds a new perspective to the complex interactions in dental implant mechanics. A two-dimensional, plane strain model of the bone was built from a CT-scan. The effect of implant contour on internal bone remodeling was investigated by considering four dental implant systems with contours similar to commercially available ones and another four with cylindrical and conical cross-sections. The remodeling algorithm predicts non-homogeneous density/elastic modulus distribution; and, implant contour has some effect on how this is distributed. Bone density is predicted to increase on the tips of the threads of the implants, but to decrease inside the grooves. Threadless implants favor to develop a softer bone around their periphery, compared to implant systems that have threads. The overall contour (dimensions and the shape) of an implant affect the bone density redistribution, but the differences between different implant systems are relatively small.

Keywords: Dental implants; Bone remodeling; Load transfer

1. Introduction

Dental implants provide an alternative for treating partial or full edentulism by serving as anchors for full-arch (Brånemark et al., 1983), partial (Jemt, 1986) and single-tooth (Lewis et al., 1988) dental prosthesis. Dental implant treatments have high survival rates (Behneke et al., 2000; Romanos and Nentwig, 2000; Khayat et al., 2001; Mordenfeld et al., 2004). Nevertheless, treatment success is influenced by location of the implant, quantity and density of bone, biomaterial aspects of the implants, and host factors such as loading and smoking (McCracken et al., 2002; Lemons, 2004). Bone–implant contact (BIC), is a measure of osseointegration of an implant. Berglundh et al. (2003) find osseointegration to be a dynamic process with *establishment* and *maintenance* phases; while the establishment phase involves continuous interplay between bone resorption and formation, in the maintenance phase osseointegration is secured through continuous adaptation to function. Many studies of implant-to-bone load transfer, in fact model the maintenance phase, and use the criteria that excessively high or inadequately low stress levels in the bone result in pathologic bone loss. A review of the finite-element method in implant dentistry is given by Geng et al. (2001).

Prosthetic attachments can be connected to the implant immediately following surgical placement, or after osseointegration takes place depending on the decision of timing of the loading. Excessive relative motion of the implant–bone interface (micromotion) indicates formation of soft connective tissue rather than a bony interface (Brunski et al., 1979); and, therefore a common healing protocol recommends a healing period on the order of a few months, during which no functional load is applied on the implant. On the other hand, immediate functional loading is possible if micromotion can be prevented during the healing period (Jaffin et al., 2000). Histomorphometric investigations of immediately loaded dental implants in human patients, which were deemed successful from a clinical point of view and based on radiographs, showed upon retrieval that BIC was on the order of 40–75%

*Corresponding author. Tel.: +1 617 373 4743; fax: +1 617 373 2921.
E-mail address: s.muftu@neu.edu (S. Müftü).

0021-9290/$ - see front matter © 2008 Elsevier Ltd. All rights reserved.
doi:10.1016/j.jbiomech.2008.01.032

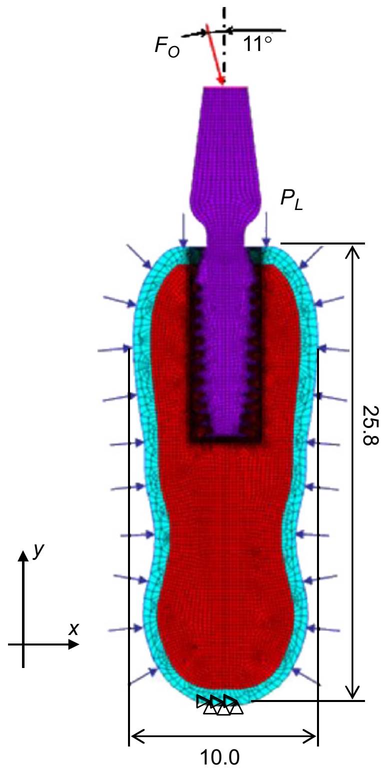

Fig. 1. Finite-element model of full abutment–implant–bone system. Fine mesh is applied near the interface of bone and implant. Occlusal load of 100 N is applied on the abutment at an angle of 11° and pressure of 500 kPa is applied on the surface of the cortical bone.

(Degidi et al., 2004, 2005; Romanos et al., 2005; Iezzi et al., 2006).

The bone near an implant is subjected to direct forces due to mastication, and long range forces due to jaw flexure. The mastication force primarily acts along the axis of the implant with a small lateral component (Graf, 1975). Magnitude of the forces generated during function and parafunction can vary greatly among individuals (Rodriguez et al., 1994). In vivo studies measured these forces in patients rehabilitated with either removable of fixed implant retained prostheses. Values ranging from 64 to 90 N for complete denture wearers to 720 N for dentate patients have been recorded (Laurell and Lundgren, 1987; Falk et al., 1989, 1990). The lateral component of the mastication force can also vary depending on the location of the tooth (Nickel et al., 2003; Koolstra, 2003). Hobkirk and Schwab (1991) showed, in patients with edentulous mandibles with osseointegrated implants, that jaw movement from the rest position results in relative displacement between the implants and force transmission between the linked components.

Bone responds by adjusting its mass density, when its mechanical loading conditions deviate from homeostatic levels, by a series of bone re/modeling processes (Frost, 1987), governed by a *physiological control system* (Hart, 2001). A (mechanical) *remodeling stimulus* is thought to be the primary control variable of this system, which includes sensor, transducer, comparator and feedback functions, and which is influenced by hormonal, metabolic, genetic and site-specific factors. Bone remodeling theories (Cowin, 1993) distinguish between *external modeling*, where bone is added or removed at the periosteal and endosteal surfaces, and *internal remodeling*, characterized by changes in apparent bone density (Cowin and Van Buskirk, 1978, 1979; Fyhrie and Carter, 1986; Frost, 1987, Huiskes et al., 1987). Stress, strain, strain energy density and fatigue microdamage have been used as the remodeling stimulus (Cowin and Hegedus, 1976; Carter et al., 1987; Huiskes et al., 1987; Cowin, 1993). In particular, the continuum level strain energy density per apparent mass density U/ρ represents the energy stored at the bone tissue level (Carter et al., 1987; Weinans et al., 1992). Despite successful predictions of cancellous bone architecture (Carter et al., 1989; Beaupré et al., 1990) and changes in bone density around a total hip arthroplasty (Weinans et al., 1993; van Rietbergen et al., 1993), adaptive remodeling has not been applied to implant dentistry. In this communication, a preliminary study of *internal remodeling* around dental implant systems (DIS) is reported.

2. Theory

Most bone remodeling theories assume that bone strives to keep a *homeostatic stimulus* (K). The rate of change of the apparent density of bone mass (ρ) is based on the difference between the *remodeling stimulus* (S) and K (Huiskes et al., 1987):

$$\frac{\mathrm{d}\rho}{\mathrm{d}t} = \begin{cases} A_{\mathrm{r}}[S - K(1+s)]^2 & \text{if } S \le K(1+s), \quad \text{(a)} \\ 0 & \text{if } K(1-s) < S < K(1+s), \quad \text{(b)} \\ A_{\mathrm{f}}[S - K(1-s)]^3 & \text{if } S \le K(1-s), \quad \text{(c)} \end{cases} \tag{1}$$

where A_{r} and A_{f} are remodeling rate constants for resorption and formation, respectively, t is time and s is the width of *dead zone*. The thresholds of bone remodeling are $K(1+s)$ and $K(1-s)$. Any remodeling stimulus in the *dead (lazy) zone* does not induce bone remodeling. Otherwise, bone hardens according to Eq. (1a) and resorbs according to (1c). The remodeling stimulus S is chosen as

$$S(x, y, t) = \frac{U(x, y, t)}{\rho(x, y, t)}, \tag{2}$$

where U is strain energy density and ρ is bone density. Carter and Hayes (1977) show that elastic modulus is related to apparent bone density and to the strain rate $\dot{\varepsilon}$ as follows:

$$E = C\dot{\varepsilon}^{0.06}\rho^3, \tag{3}$$

where $C = 3.790$. The unit of the elastic modulus E is GPa if ρ is in kg/m^3. Eq. (1) is solved by forward Euler time integration:

$$\rho^{(j)}_m = \begin{cases} \rho^{(j-1)}_m + A\Delta t[S^{(j-1)}_m - K(1+s)]^2 & \text{if } S^{(j-1)}_m \geq K(1+s), & \text{(a)} \\ 0 & \text{if } K(1-s) < S^{(j-1)}_m < K(1+s), & \text{(b)} \\ \rho^{(j-1)}_m + A\Delta t[S^{(j-1)}_m - K(1-s)]^3 & \text{if } S^{(j-1)}_m \leq K(1-s), & \text{(c)} \end{cases} \quad (4)$$

where j is the time step and m is mesh node location. Here, $A_r = A_f = A$ is assumed, and $A\Delta t$ is treated as a single-time integration parameter. Strain energy density and remodeling stimulus are computed by using the finite-element program ANSYS (Canonsburg, PA) and its APDL programming facility. Convergence is achieved when remodeling stimuli of all bone elements fall into the dead zone. In this work the effect of strain rate is neglected, and the algorithm is restricted to the range $1\,\text{kPa} \leqslant E \leqslant 13\,\text{GPa}$.

3. Methods

A two-dimensional bone contour of the mandibular premolar region obtained form a CT-scan was assigned 1 mm thick outer cortical layer ($E = 13\,\text{GPa}$). The model was discretized using Plane42 elements, with the plane strain option. A fine mesh was applied in the vicinity of the bone–implant interface (Fig. 1). On average, the number of elements for the implant systems, cortical bone, and internal bone region were 2800, 1000, and 9000, respectively. All materials were assumed linear-elastic, homogenous, and isotropic. Elastic modulus (E) and Poisson's ratio (v) are 113.8 GPa and 0.3 (Lemons and Dietsh-Misch, 1999), respectively, for titanium implant system. Poisson's ratio of the bone is 0.3 (Martin et al., 1998). The first group of implants (Fig. 2) includes four DIS, which are similar to four commercially available implant systems (Chou, 2007). The second group of implants (Fig. 3) includes four simple geometric shapes: a

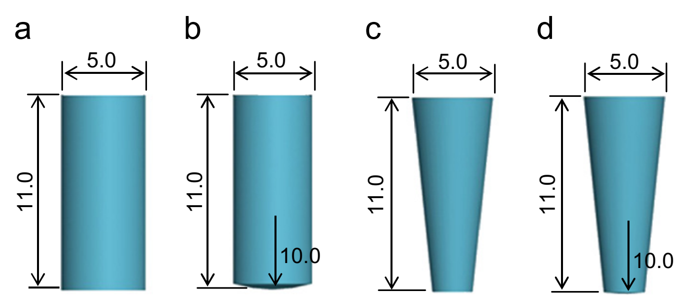

Fig. 3. Dimensions of four hypothetic implants in mm.

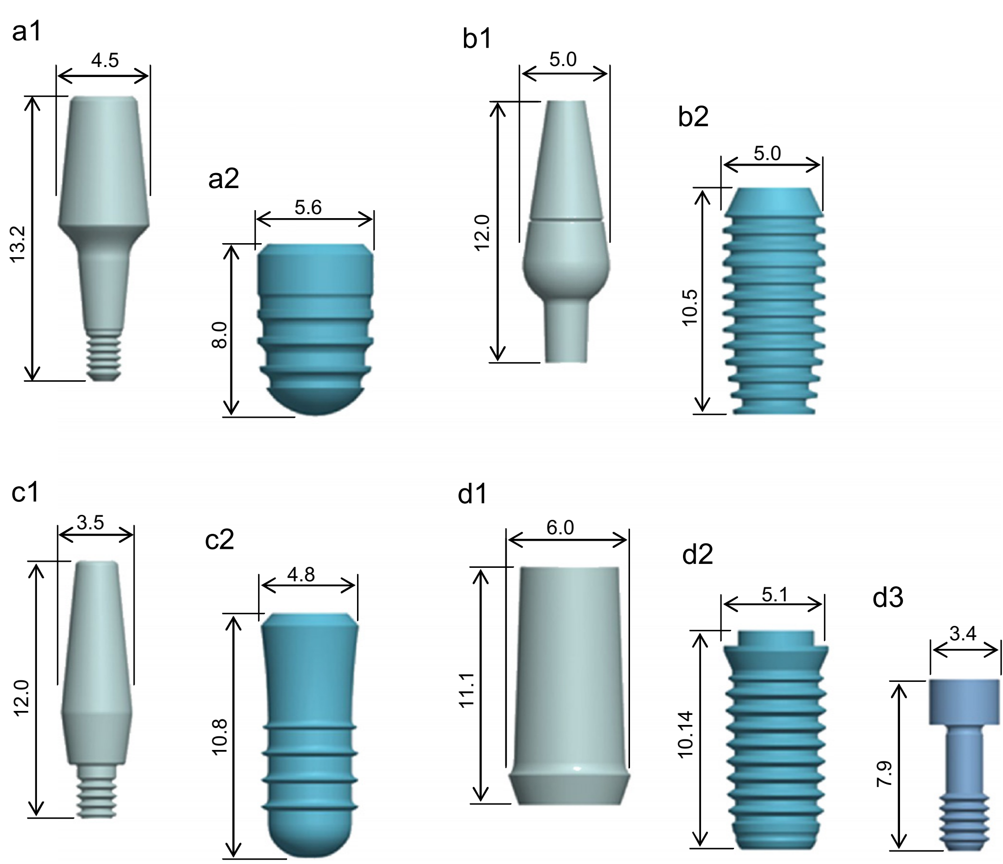

Fig. 2. Four commercially available dental implant systems: (a) DIS-1, Ankylos; (b) DIS-2, Bicon; (c) DIS-3, ITI; and (d) DIS-4, Nobel Biocare. All dimensions are shown in mm.

Please cite this article as: Chou, H.Y., et al., Predictions of bone remodeling around dental implant systems. Journal of Biomechanics (2008), doi:10.1016/j.jbiomech.2008.01.032

straight cylinder, a straight cylinder with rounded end, a truncated cone, and a truncated cone with rounded end.

In this study, we consider the short range (F_O) and long range (P_L) external loads on the system (Fig. 1). Mastication force was modeled as a concentrated force, $F_O = 100\,\text{N}$, applied on the abutment, in the buccal-lingual plane (BL plane) at 11° (Graf, 1975). The long range force P_L is applied on the outer periphery of the cortical bone, to simulate the effect of mandibular flexure (Hobkirk and Schwab, 1991).

The parameters of the model are K, s, $A\Delta t$, and P_L. These parameters were determined based on extensive numerical experiments as described by Chou (2007). The parameters were varied until realistic-looking bone density distributions were predicted by the model. The values used in this work were thus chosen as $K = 25\,\text{N m/kg}$, $s = 0.65$, $P_L = 500\,\text{kN/m}$, $A\Delta t = 5\times10^{-3}\,(\text{kg}^4/\text{N m}^4)$. The initial internal bone density was assumed to be $\rho(x,y,0) = 808\,\text{kg/m}^3$ ($E = 2.0\,\text{GPa}$). The mandible is constrained in x- and y-directions at the bottom (Fig. 1).

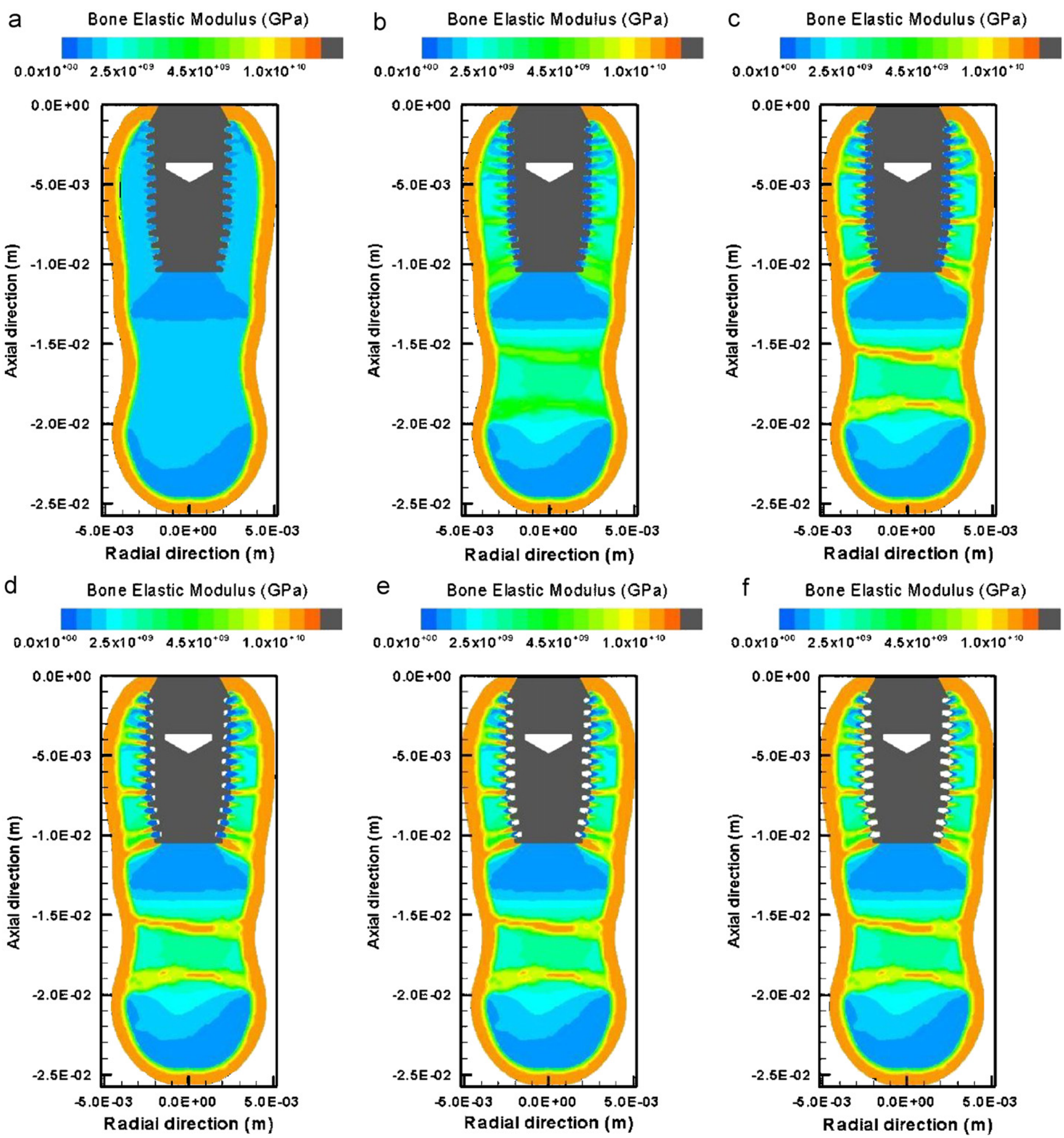

Fig. 4. Iterative changes of elastic modulus distribution around a dental implant. Total number of iteration steps for this case to achieve converged result is 1317. (a–f) represent iteration levels 1,40,100,250,300, and 1317.

Table 1
Iterative changes of average bone density in trabecular section for the case presented in Fig. 4

Time step	0	1	40	100	250	300	1317
Ave. density in Tra. Sec., ρ_{ave}^{Tra} (kg/m^3)	808	813.22	877.06	909.42	883.12	879.24	875.13
E (GPa)	1.95	1.99	2.49	2.78	2.55	2.51	2.48
Ave. remodeling stimulus, S_{ave}	N/A	40.89	27.45	21.39	21.76	21.78	21.79

Elastic modulus is computed according to Eq. (3).

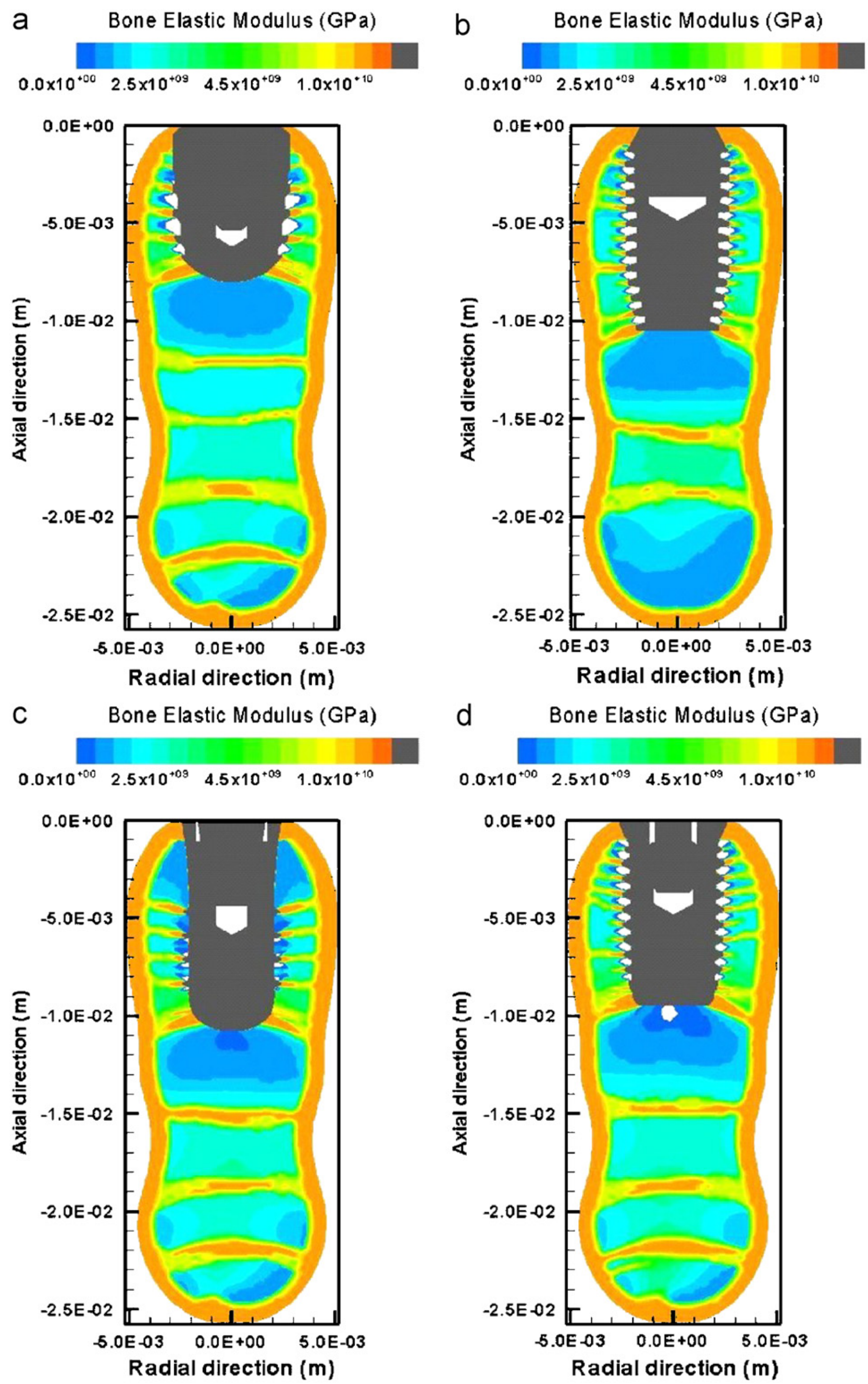

Fig. 5. Elastic moduli distribution of four commercially available implant systems with 100 N occlusal load applied on the implant and $P_L = 500$ kN/m. Note that the algorithm predicts horizontally oriented, high-density bone regions connecting cortical sections, in addition to bone densification and resorption around implants.

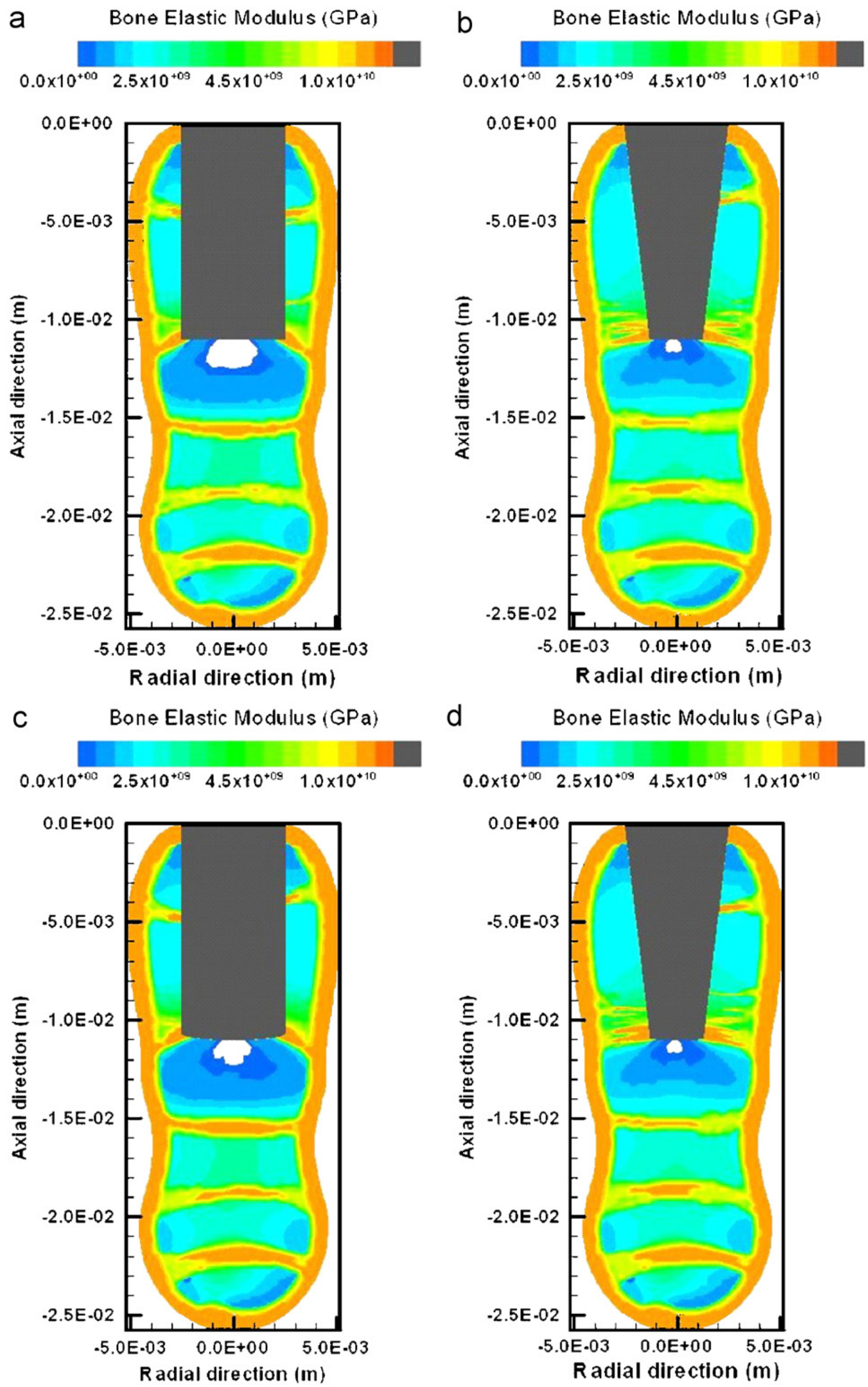

Fig. 6. Elastic moduli distribution of four hypothetic implant systems with 100 N occlusal load applied on the implant and $P_L = 500$ kN/m. Note that the algorithm predicts horizontally oriented, high-density bone regions connecting cortical sections in addition to bone, densification and resorption around implants.

4. Results

The iterative change of bone modulus in the internal remodeling region is presented in Fig. 4. The colors from blue to orange indicate the range $1 \leqslant E \leqslant 13$ GPa, or cancellous to cortical bone. White represents total bone resorption ($E = 1$ kPa). In the first 100 steps bone gradually develops high modulus regions, with values comparable to cortical bone. After 100 iterations, no significant update takes place except inside the grooves of

Table 2
Average bone density in internal remodeling region at steady state

	DIS-1	DIS-2	DIS-3	DIS-4
$\rho_{\mathrm{ave}}^{\mathrm{Tra}}$ (kg/m^3)	936.86	875.21	949.14	921.43
	Straight cylinder	Root form	Cylinder with rounded end	Root form with rounded end
$\rho_{\mathrm{ave}}^{\mathrm{Tra}}$ (kg/m^3)	925.60	945.35	934.73	946.82

the implant, where bone resorption is significant. Table 1 shows the average bone density increases in earlier iteration steps, where bone formation is more active; and it decreases when bone resorbs inside the grooves. The convergence was reached in 1317 iterations.

The homeostatic bone modulus distributions for DIS-1–4 are presented in Fig. 5, and those for the four simple geometric shapes are presented in Fig. 6. The average bone densities at homeostatic equilibrium are summarized in Table 2. Figs. 5 and 6 show the redistribution of the bone mass. Below the implants, the algorithm predicts horizontally oriented regions of high-density bone, connecting the cortical sections by traversing the BL cross-section. We see four of these regions for DIS-1, three for DIS-3, and -4 and two for DIS-2. Around the apical sections of all implant types, the bone density increases and the high-density regions connect to the cortical bone.

For the smooth surface implant designs (Fig. 6, Table 2), the activity of bone formation is not as prominent as in DIS-1–4, but the overall elastic modulus distribution still shows bone densification. The implant is supported at its apical section by a wider area of hard bone, but, in general, more bone resorption is predicted immediately below the implant (Fig. 6). Bone densification is less pronounced for the implants with smooth surfaces (Fig. 6) along the implant axis, whereas implants in Fig. 5 develop high bone density near tips of the threads. The model predicts shielding of the bone in the grooves from proper stimulation.

5. Discussion

The internal stress distribution in the mandible is affected not only by forces on the teeth, but also by the forces applied on the mandible by the muscles of the masticatory system, due to various opening and closing actions required by chewing, speech, and involuntary jaw motions. Hobkirk and Schwab (1991) have demonstrated, in subjects with edentulous mandibles containing osseointegrated implants, that jaw movement from the rest position results in relative displacement between the linked implants of up to 420 μm and force transmission between the linked implants of up to 16 N.

Determination of the muscle forces presents a complicated problem, which requires information on the muscle activity levels, which are further complicated if mastication is taking place (Koolstra and van Eijden, 1999; Müftü and Müftü, 2006). The internal stresses in the mandible, therefore, can have a very complicated distribution (Hart et al., 1992; Korioth and Hannam, 1994; Vollmer et al., 2000; Hirayabashi et al., 2002). In this work, the internal stress distribution is simulated by the external distributed load P_L (Chou, 2007). This simplification will be improved in our future work, where the internal stress distribution will be calculated from more detailed analyses.

Nevertheless, interesting general observations can be made; including the effect that threads have on bone remodeling, where bone density is predicted to increase on the tips of the threads but to decrease inside the grooves; Threadless implants develop softer bone around their periphery, compared to implant systems that have threads; The overall contour of an implant affects the bone density redistribution. This communication presents the first step toward the complex problem of bone remodeling around DIS, which in the future should be analyzed with coordinated in vivo experiments and mathematical modeling. Such an approach can then be expected to contribute to our understanding of mechanotransduction, in general, and to design of improved implant systems, in particular.

Conflict of interest

The authors had no conflict of interest in working on or writing this article.

Acknowledgment

This work was supported in part by a research grant provided to Northeastern University by Bicon Dental Implants (Boston, MA).

References

Beaupré, G.S., Orr, T.E., Carter, D.R., 1990. An approach for time-dependent bone modeling and remodeling—a preliminary remodeling simulation. Journal of Orthopaedic Research 8, 662–670.

Behneke, A., Behneke, N., d'Hoedt, B., 2000. The longitudinal clinical effectiveness of ITI solid-screw implants in partially edentulous patients: a 5-year follow-up report. International Journal of Oral & Maxillofacial Implants 15, 633–645.

Please cite this article as: Chou, H.Y., et al., Predictions of bone remodeling around dental implant systems. Journal of Biomechanics (2008), doi:10.1016/j.jbiomech.2008.01.032

Berglundh, T., Abrahamsson, I., Lang, N.P., Lindhe, J., 2003. De novo alveolar bone formation adjacent to endosseous implants. Clinical Oral Implants Research 14, 251–262.

Brånemark, P.-T., Adell, R., Albrektsson, T., Lekholm, U., Lundkvist, S., Rockler, B., 1983. Osseointegrated titanium fixtures in the treatment of edentulousness. Biomaterials 4, 25–28.

Brunski, J.B., Moccia Jr., A.F., Pollack, S.R., Korostoff, E., Trachtenberg, D.I., 1979. The influence of functional use of endosseous dental implants on the tissue implant interface. Journal of Dental Research 58, 1953–1969.

Carter, D.R., Hayes, W.C., 1977. The behavior of bone as a two-phase porous structure. Journal of Bone and Joint Surgery 59A, 954–962.

Carter, D.R., Fyhrie, D.P., Whalen, R.T., 1987. Trabecular bone density and loading history: regulation of connective tissue biology by mechanical energy. Journal of Biomechanics 20, 785–794.

Carter, D.R., Orr, T.E., Fyhrie, D.P., 1989. Relationships between loading history and femoral cancellous bone architecture. Journal of Biomechanics 22, 231–244.

Chou, H.Y., 2007. Numerical evaluation of mechanotransduction in bone remodeling around dental implants. M.S. Thesis, Northeastern University, Boston, MA.

Cowin, S.C., 1993. Bone stress adaptation models. Journal of Biomechanical Engineering 115, 528–533.

Cowin, S.C., Hegedus, D.H., 1976. Bone remodeling 1: theory of adaptive elasticity. Journal of Elasticity 6, 313–326.

Cowin, S.C., Van Buskirk, W.C., 1978. Internal bone remodeling induced by a medullary pin. Journal of Biomechanics 11, 269–275.

Cowin, S.C., Van Buskirk, W.C., 1979. Surface bone remodeling induced by a medullary pin. Journal of Biomechanics 12, 269–276.

Degidi, M., Scarano, A., Piattelli, M., Piatelli, A., 2004. Histologic evaluation of an immediately loaded titanium implant retrieved from a human after 6 months in function. Journal of Oral Implantology 30, 289–296.

Degidi, M., Scarano, A., Iezzi, G., Piattelli, A., 2005. Histologic analysis of an immediately loaded implant retrieved after 2 months. Journal of Oral Implantology 31, 247–254.

Falk, H., Laurell, L., Lundgren, D., 1989. Occlusal force pattern in dentitions with mandibular implant-supported fixed cantilever prostheses occluded with complete dentures. International Journal of Oral & Maxillofacial Implants 4, 55–62.

Falk, H., Laurell, L., Lundgren, D., 1990. Occlusal interferences and cantilever joint stress in implant-supported prostheses occluding with complete dentures. International Journal of Oral & Maxillofacial Implants 5, 70–77.

Frost, H.M., 1987. Bone "Mass" and the "Mechanostat": a proposal. The Anatomical Record 219, 1–9.

Fyhrie, D.P., Carter, D.R., 1986. A unifying principle relating stress to trabecular bone morphology. Journal of Orthopaedic Research 4, 304–317.

Geng, J.P., Tan, K.B.C., Liu, G.R., 2001. Application of finite element analysis in implant dentistry: a review of the literature. Journal of Prosthetic Dentistry 85, 585–598.

Graf, H., 1975. Occlusal forces during function. In: Rowe, A. (Ed.), Proceedings of Symposium on Occlusion: Research on Form and Function. University of Michigan School of Dentistry, Ann Arbor, pp. 90–111.

Hart, R.T., 2001. Bone modeling and remodeling theories and computation. In: Cowin, S.C. (Ed.), Bone Mechanics Handbook, second ed. CRC Press, Boca Raton, FL, pp. 31-1–31-42.

Hart, R.T., Henebbel, V., Thongpreda, N., van Buskirk, W.C., Anderson, R.C., 1992. Modeling the biomechanics of the mandible: a three dimensional finite element study. Journal of Biomechanics 25, 261–286.

Hirayabashi, M., Motoyoshi, M., Ishimaru, T., Kasai, K., Namura, S., 2002. Stress in mandibular cortical bone during mastication: biomechanical considerations using a three dimensional finite element method. Journal of Oral Science 44, 1–6.

Hobkirk, J.A., Schwab, J., 1991. Mandibular deformation in subjects with osseointegrated implants. International Journal of Oral & Maxillofacial Implants 6, 319–328.

Huiskes, R., Weinans, H., Grootenboer, H.J., Dalstra, M., Fudala, B., Slooff, T.J., 1987. Adaptive bone-remodeling theory applied to prosthetic-design analysis. Journal of Biomechanics 20, 1135–1150.

Iezzi, G., Pecora, G., Scarano, A., Perrotti, V., Piatelli, A., 2006. Histologic evaluation of 3 retrieved immediately loaded implants after a 4-month period. Implant Dentistry 15, 305–312.

Jaffin, R.A., Kumar, A., Berman, C.L., 2000. Immediate loading of implants in partially and fully edentulous jaws: a series of 27 case reports. Journal of Periodontology 71, 833–838.

Jemt, T., 1986. Modified single and short-span restorations supported by osseointegrated fixtures in the partially edentulous jaw. Journal of Prosthetic Dentistry 55, 243–247.

Khayat, P.G., Hallage, P.G.H., Toledo, R.A., 2001. An investigation of 131 consecutively placed wide screw-vent implants. International Journal of Oral & Maxillofacial Implants 16, 827–832.

Koolstra, J.H., 2003. Number crunching with the human masticatory system. Journal of Dental Research 82, 672–676.

Koolstra, J.H., van Eijden, T.M.G.J., 1999. Three dimensional dynamical capabilities of the human masticatory muscles. Journal of Biomechanics 32, 145–152.

Korioth, T.W.P., Hannam, A.G., 1994. Mandibular forces during simulated tooth clenching. Journal of Orofacial Pain 8, 178–189.

Laurell, L., Lundgren, D., 1987. Interfering occlusal contacts and distribution of chewing and biting forces in dentitions with fixed cantilever prostheses. Journal of Prosthetic Dentistry 58, 626–632.

Lemons, J.E., 2004. Biomaterials, biomechanics, tissue healing, and immediate-function dental implants. Journal of Oral Implantology 30, 318–324.

Lemons, J.E., Dietsh-Misch, F., 1999. Biomaterials for dental implants. In: Misch, C.E. (Ed.), Contemporary Implant Dentistry, second ed. Mosby, St. Louis, pp. 271–302.

Lewis, S.G., Beumer, J., Perri, G.R., Hornburg, W.P., 1988. Single tooth implant supported restorations. International Journal of Oral & Maxillofacial Implants 3, 25–30.

Martin, R.B., Burr, D.B., Sharkey, N.A., 1998. Skeletal Tissue Mechanics. Springer, New York, 131pp.

McCracken, M., Lemons, J.E., Jeffcoat, M., Koth, D.L., Fritz, M.E., 2002. Histomorphological evaluation of loaded plate-form and root-form implants in Macaca mulatta monkeys. Clinical Oral Implants Research 13, 214–220.

Mordenfeld, M.H., Johansson, A., Hedin, M., Billström, C., Fyberg, K.A., 2004. A retrospective clinical study of wide-diameter implants used in posterior edentulous areas. International Journal of Oral & Maxillofacial Implants 19, 387–392.

Müftü, S., Müftü, A., 2006. Biomechanics of tooth and jaw. In: Webster, J.G. (Ed.), Encyclopedia of Medical Devices and Instrumentation. Wiley, NY, pp. 411–428.

Nickel, J.C., Iwasaki, L.R., Walker, R.D., McLanchlan, K.R., McCall Jr., W.D., 2003. Human masticatory muscle forces during static biting. Journal of Dental Research 82, 212–217.

Rodriguez, A.M., Aquilino, S.A., Lund, P.S., 1994. Cantilever and implant biomechanics: a review of the literature, part 1. Journal of Prosthodontics 3, 41–46.

Romanos, G.E., Nentwig, G.H., 2000. Single molar replacement with a progressive thread design implant system: a retrospective clinical report. International Journal of Oral & Maxillofacial Implants 15, 831–836.

Romanos, G.E., Testori, T., Degidi, M., Piatelli, A., 2005. Histologic and histomorphometric findings from retrived, immediately occlusally loaded implants in humans. Journal of Periodontology 76, 1823–1832.

van Rietbergen, B.V., Huiskes, R., Weinans, H., Sumner, D.R., Turner, T.M., Galante, J.O., 1993. The mechanism of bone remodeling and resorption around press-fitted THA stems. Journal of Biomechanics 26, 369–382.

Please cite this article as: Chou, H.Y., et al., Predictions of bone remodeling around dental implant systems. Journal of Biomechanics (2008), doi:10.1016/j.jbiomech.2008.01.032

Vollmer, D., Meyer, U., Joos, U., Vegh, A., Piffko, J., 2000. Experimental and finite element study of a human mandible. Journal of Cranio-Maxillofacial Surgery 28, 91–96.

Weinans, H., Huiskes, R., Grootenboer, H.J., 1992. Effects of material properties of femoral hip components on bone remodeling. Journal of Orthopaedic Research 10, 845–853.

Weinans, H., Huiskes, R., van Rietbergen, B.V., Sumner, D.R., Turner, T.M., Galante, J.O., 1993. Adaptive bone remodeling around bonded noncemented total hip arthroplasty: a comparison between experiments and computer simulation. Journal of Orthopaedic Research 11, 500–551.

Please cite this article as: Chou, H.Y., et al., Predictions of bone remodeling around dental implant systems. Journal of Biomechanics (2008), doi:10.1016/j.jbiomech.2008.01.032